Photorefractive ring resonator with seeding as an externally driven oscillator

Svetlana A. Tatarkova,[1,*] Malgosia Kaczmarek,[1,†] Changxi Yang,[1,‡] and Robert W. Eason[2]
[1]*School of Physics, University of Exeter, Stocker Road, Exeter EX4 4QL, United Kingdom*
[2]*Optoelectronics Research Centre and Department of Physics and Astronomy, University of Southampton, Southampton S017 1BJ, United Kingdom*

(Received 24 May 2002; published 11 October 2002)

We report on experimental and theoretical studies of a photorefractive ring resonator pumped by a 1.06 μm beam and injected with a weak, external, seeding beam. The competition between the two dominant gratings that form inside the photorefractive crystal leads to characteristic periodic oscillations in the intensity of the resonating beam, which originate from the frequency difference between the pump beam and the unidirectional oscillation beam. We show that such a system can be treated as a driven nonlinear oscillator.

DOI: 10.1103/PhysRevA.66.043807 PACS number(s): 42.65.Hw, 42.65.Sf

The unidirectional photorefractive ring resonator [1] (PRR) has been extensively studied recently because of a wide variety of nonlinear effects [1–3]. The complicated dynamics due to spatial-temporal instabilities and mode competition makes the theoretical modeling of such systems quite difficult. Extended analysis involving the transverse field components is usually needed to describe satisfactorily the pattern formation and pattern evolution [5,6]. If the ring resonator is adjusted to low Fresnel number and operates in the basic Gaussian mode, alternation of modal patterns might occur spontaneously, caused by thermal variations of the cavity length [3,4]. In this paper we report experimental evidence of temporal field variation that originates from oscillator dynamics rather then thermal instabilities. A periodic intensity modulation was observed that was stable in time and had fixed amplitude and period of modulation when other parameters were kept unchanged. The period of the modulation depends on the incident angle of the pumping beam and the crystal orientation relative to the resonator axis. Similar periodic instabilities were observed in a more complicated experimental arrangement of a self-pumped phase-conjugated mirror with four-beam mixing [7]. Although the physics is essentially the same, we demonstrate the experimental observation of this phenomenon in a photorefractive ring resonator and discuss the conditions on frequency detuning.

Photorefractive resonators rely on two-beam coupling (TBC) and/or phase conjugation to provide energy for the oscillations inside the cavity. Uniquely in these resonators, the oscillation beam can build up almost regardless of the optical cavity length with frequency determined by the round-trip phase condition [1]. In typical ring resonator geometry, a pump beam incident on a photorefractive crystal placed inside the cavity induces scattered light, which can give rise to self-sustained oscillations. The oscillations start from this scattered light and get amplified through subsequent TBC interaction with the pump beam in the photorefractive crystal. The oscillation beam builds up if the TBC gain is above threshold, that is, when gains exceed losses, and can reach a high intensity even with moderate TBC amplification provided the cavity losses, including the crystal's absorption, are small [8]. In this configuration, light propagation inside a cavity should be unidirectional, as the TBC gain is directional, determined by the crystal's symmetry, alignment, and charge-transport properties.

If the resonator is below the threshold the oscillation will decay. This happens when the TBC gain (coupling coefficient) is too small or the scattered light is too weak to overcome the cavity losses. In this case, the injection of an external weak seeding beam can serve as a support to develop the resonator oscillation by creating additional scattering photons. However, we have obtained experimental evidence of periodic oscillation in the resonator output. The factor causing instabilities is grating competition. The injected seeding beam forms a stationary grating with the pump beam. The other, moving, grating arises due to TBC and the resonator round-trip phase conditions. Then the resonator beam starts to diffract on both gratings which leads to instabilities. This resonator is mathematically equivalent to the driven nonlinear oscillator and can be described well by a simple mathematical model.

In this paper we present a study of the dynamic properties of a nonlinear oscillator based on a running-wave PRR, which shows a self-sustained oscillation in the frequency different from that of the pump beam [1]. The model we present provides an explanation of the periodic variation in the output intensity of the resonating beam. The presence of an external, weak seeding beam injected into the resonator contributes to beating between the different optical frequencies that compose the resonating beam. We show that the beating frequency depends on such resonator parameters as the pump incident angle and crystal orientation.

Let us consider a one-dimensional model of the PRR with an external seeding beam oscillating in a single-resonator mode. We assume that the uniform pump electric field can be presented as

*Corresponding author. Present address: School of Physics and Astronomy, University of St. Andrews, St. Andrews KY16 9SS, Scotland. Email address: sat3@st-andrews.ac.uk

†Present address: Department of Physics and Astronomy, University of Southampton, Southampton S017 1BJ, United Kingdom. Email address: mfk@soton.ac.uk

‡Present address: Department of Precision Instruments, Tsinghua University, Beijing, China.

$$\mathbf{E}_P(\mathbf{r},t)=\mathbf{E}_P\exp[i(\mathbf{k}_P\cdot\mathbf{r}-\omega_P t)]+\text{c.c.}, \tag{1}$$

where $\mathbf{E}_P(t)$ is the slowly varying pump amplitude, and $\mathbf{k}_P$ and ω_P are the wave vector and frequency, respectively. The electric field inside the resonator is assumed to consist of two components:

$$\mathbf{E}(\mathbf{r},t)=\mathbf{E}_R(\mathbf{r},t)+\mathbf{E}_S(\mathbf{r},t), \tag{2}$$

where $\mathbf{E}_R(\mathbf{r},t)$ and $\mathbf{E}_S(\mathbf{r},t)$ are the resonator and seeding-beam electric-field components, respectively, which can be assumed to have the same form as the pump beam:

$$\mathbf{E}_R(\mathbf{r},t)=\mathbf{E}_R(t)\exp[i(\mathbf{k}\cdot\mathbf{r}-\omega t)]+\text{c.c.}, \tag{3}$$

$$\mathbf{E}_S(\mathbf{r},t)=\mathbf{E}_S\exp[i(\mathbf{k}_S\cdot\mathbf{r}-\omega_P t)]+\text{c.c.}, \tag{4}$$

where $\mathbf{k}$ is the passive-resonator wave vector, ω is the passive-resonator frequency, and $|\mathbf{k}_S|=|\mathbf{k}_P|$.

We have chosen the resonator mode as well as the pump and seeding waves to be uniform plane waves for simplicity. Also we use the mean-field limit, in which we neglect the amplitude variation along the cavity length. Moreover, we also assume the weak-field limit, i.e., the total intensity of the resonator field is far less than that of the pump beam $I_S, I_R \ll I_P$. Finally, we take all beams to have the same, extraordinary polarization. They all propagate at small angles versus each other and along the cavity axis.

Considering a unidirectional ring cavity having a lossy medium with conductivity σ, which we also adjust to give damping due to cavity imperfections and reflector transmission and diffraction, we can write an equation for the resonator field as follows [9]:

$$\nabla^2\mathbf{E}_R-\mu_0\sigma\frac{\partial\mathbf{E}_R}{\partial t}-\mu_0\epsilon\frac{\partial^2\mathbf{E}_R}{\partial t^2}=-\frac{1}{\epsilon}\boldsymbol{\nabla}(\boldsymbol{\nabla}\cdot\mathbf{P}_{\text{NL}})+\mu_0\frac{\partial^2\mathbf{P}_{\text{NL}}}{\partial t^2}, \tag{5}$$

where $\mathbf{P}_{\text{NL}}(\mathbf{r},t)$ is the nonlinear polarization of the photorefractive medium induced by contributions from all field components inside the crystal. We neglect here the term $\boldsymbol{\nabla}\cdot\mathbf{P}_{\text{NL}}\approx 0$, which is due to the effect of dispersion. Taking into account our assumptions we determine the nonlinear polarization as

$$\begin{aligned}\mathbf{P}_{\text{NL}}(\mathbf{r},t)&=2\epsilon_0\{\mathbf{E}_P(\mathbf{r},t)+\mathbf{E}(\mathbf{r},t)\}\Delta n(\mathbf{r},t)\\&\approx 2\epsilon_0\mathbf{E}_P(\mathbf{r},t)\Delta n(\mathbf{r},t),\end{aligned} \tag{6}$$

where $\Delta n(\mathbf{r},t)$ is the refractive index change in the photorefractive material. This photoinduced change in the refractive index, Δn, is created by the interference pattern between all the incident (pump and seeding) and resonator beams:

$$\begin{aligned}I(\mathbf{r},t)&=\frac{1}{2}[\mathbf{E}_P(\mathbf{r},t)+\mathbf{E}_R(\mathbf{r},t)+\mathbf{E}_S(\mathbf{r},t)]^2\\&=I_0(t)\left[1+\left(\frac{\mathbf{E}_P\mathbf{E}_R^*}{I_0}\exp[i(\Delta\mathbf{k}\cdot\mathbf{r}-\Delta\omega t)]+\text{c.c.}\right)\right.\\&\quad\left.+\left(\frac{\mathbf{E}_P\cdot\mathbf{E}_S^*}{I_0}\exp[i\Delta\mathbf{k}_P\cdot\mathbf{r}]+\text{c.c.}\right)\right]\\&=I_0(t)+I_1(\mathbf{r},t)+I_2(\mathbf{r},t),\end{aligned} \tag{7}$$

where $\Delta\mathbf{k}=\mathbf{k}_P-\mathbf{k}$, $\Delta\mathbf{k}_P=\mathbf{k}_P-\mathbf{k}_S$, $\Delta\omega=\omega_P-\omega$, and $I_0(t)=|\mathbf{E}_P|^2+|\mathbf{E}_R|^2+|\mathbf{E}_S|^2$. We assumed that the interference between the resonator and seeding beams as well as terms with higher frequencies such as $2\omega_p$ are negligible due to the much smaller grating amplitude and the assumption made earlier of the weak-field limit.

The modulated terms, namely, the second (I_1) and third (I_2) terms are particularly interesting. I_1 is responsible for creating a moving grating and I_2 for forming a stationary interference pattern between the pump and the seeding beams. So the resonator beam is built on the existing diffraction pattern formed by pump- and seeding-beam interference.

The time evolution of Δn as a function of intensity modulation arises from the theory of Kukhtarev [10,11] and is given by

$$\left[\frac{\partial}{\partial t}+\frac{1}{\tau}\right]\Delta n(\mathbf{r},t)=i\Gamma\{I_1(\mathbf{r},t)+I_2(\mathbf{r},t)\}, \tag{8}$$

where $\Gamma=\gamma n_{\text{st}}^3 r_{\text{eff}}/2I_P\tau_c$, γ is the complex coupling constant, τ is the intensity-dependent time constant, $\tau_c=\tau I_0/I_P$ is a time constant, n_{st} is the static index of refraction, and r_{eff} is the effective electro-optic coefficient of the crystal. We assume the solution of this equation to be of the following form, namely, a linear superposition of two separate terms:

$$\begin{aligned}\Delta n(\mathbf{r},t)&=Q_1(t)\exp[i(\Delta\mathbf{k}\cdot\mathbf{r}-\Delta\omega t)]\\&\quad+Q_2(t)\exp[i\Delta\mathbf{k}_P\mathbf{r}]+\text{c.c.},\end{aligned} \tag{9}$$

where $Q_1(t)$ and $Q_2(t)$ are two slowly varying components of the index-grating complex amplitude. Substituting into Eq. (8) for the refractive index change we obtain the equations for the grating amplitudes:

$$\begin{aligned}\frac{dQ_1}{dt}&=-\left[-\frac{1}{\tau}-i\Delta\omega\right]Q_1+i\Gamma(\mathbf{E}_P\cdot\mathbf{E}_R^*),\\\frac{dQ_2}{dt}&=-\frac{1}{\tau}Q_2+i\Gamma(\mathbf{E}_P\cdot\mathbf{E}_S^*).\end{aligned} \tag{10}$$

From these equations describing the time development of the index grating, we can see that one component of its amplitude (Q_1) will oscillate at the difference frequency and decay in time when the pump is blocked. The other, stationary, component (Q_2) decays smoothly in time when the pump is blocked. The steady-state grating amplitudes depend on the seeding/resonator beam ratio and coupling coefficient. When the resonator beam builds up, the ratio of grating amplitudes is fixed and equal to the ratio of seeding/resonator beam intensities.

Let us go back to the field equation (5). We assume that the variations in the field intensity transverse to the resonator axis are slowly varying compared to the optical wavelengths and hence we can neglect the transverse derivatives. Substituting Eq. (3) for the electric-field component into the wave equation (5), assuming that the fictional conductivity σ indeed corresponds the resonator's quality, defined by [9]

$$\sigma=\varepsilon_0\frac{\omega}{Q_R}, \tag{11}$$

and multiplying through by $\exp[-i(\mathbf{k}\cdot\mathbf{r}-\omega t)]$, we obtain the wave equation of the resonator field as

$$\frac{d\mathbf{E}_R}{dt}=-\frac{1}{2}\frac{\omega}{Q_R}\mathbf{E}_R-\frac{\mu_0}{2\omega L_R}\mathrm{Im}\left(\int_0^{L_R}\exp[-i(\mathbf{k}\cdot\mathbf{r}-\omega t)]\frac{\partial^2\mathbf{P}_{\mathrm{NL}}}{\partial t^2}dz\right), \tag{12}$$

where L_R is the resonator's length and the integration is carried out over this length. Substituting the expression for the nonlinear polarization (6) together with Eq. (9) into the resonator field equation (12), we obtain

$$\frac{d\mathbf{E}_R}{dt}=-\frac{\omega}{2Q_R}\mathbf{E}_R+\alpha\mathbf{E}_P Q_1^*+\beta\mathbf{E}_P Q_2^*\sin(\Delta\omega t), \tag{13}$$

where

$$\alpha=\frac{\mu_0\varepsilon_0\omega l}{L_R},$$

$$\beta=\frac{\mu_0\varepsilon_0\omega_P^2}{\omega L_R}\frac{2\sin[(\mathbf{k}_S-\mathbf{k})l/2]}{\mathbf{k}_S-\mathbf{k}}\equiv\frac{\mu_0\varepsilon_0\omega_P^2}{\omega L_R}l,$$

and l is the interaction length in the crystal.

The normalized form ($E'=E_R/E_P$) for the resonator field can be expressed as

$$\frac{dE'}{dt}=-\frac{1}{2}\frac{\omega}{Q_R}E'+\alpha Q_1^*+\beta Q_2^*\sin(\Delta\omega t). \tag{14}$$

This is the equation for a driven nonlinear oscillator. The numerical simulations of this equation are well known [9] and show periodic evolution of the resonator field depending on the intensity of the seeding signal.

We have shown here that injection of an external seeding beam into the resonator cavity makes the cavity behave like a driven nonlinear oscillator with its output intensity periodically oscillating with amplitude depending on the ratio of the stationary to moving grating amplitude. If the resonator gain is high so that the oscillating grating has an amplitude two or more orders of magnitude greater than that of the stationary grating, the periodic modulation will be suppressed by the strong resonator field. The frequency of the periodic output corresponds to the beat frequency between the pump and resonator beams. In the case when the intensity of the injected beam is zero, then the equation goes to that of the typical "free" oscillator case, described in detail by, for example, Anderson and Saxena [12] and Jost and Saleh [11]. The other special case is when $\Delta\omega=0$ and there is no frequency shift between the oscillating mode and the pump and no modulation effect.

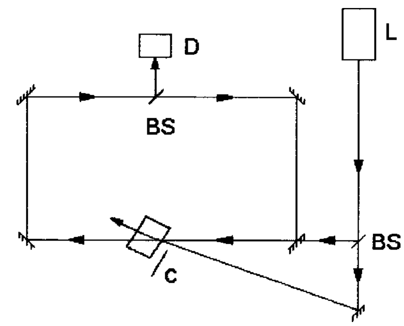

FIG. 1. Photorefractive ring resonator geometry with an additional seeding beam. BS, beam splitter; *L*, laser; *c*, direction of crystal axis.

In our experiment we used a sample of Rh:$BaTiO_3$ doped with 3200 ppm of rhodium added to the melt ($6\times5\times5\ \mathrm{mm}^3$) pumped by a single-longitudinal-mode 1.06 μm miniature neodymium-doped yttrium aluminum garnet (Nd:YAG) laser. The laser output beam was split into pump and seeding beams. Four mirrors, three of them with high reflectivity (99.9%) and one with 90% reflectivity, formed the ring resonator. The seeding beam was injected into the cavity through this $R=90\%$ mirror. The pump-beam power was kept constant at 100 mW and the seeding-beam power was varied in the range from 16 mW to 16 μW. Both beams had extraordinary polarization.

We varied the level of amplification inside the cavity by changing the coupling coefficient, namely, by either changing the incident angle of the pump beam or reorienting the crystal itself relative to the resonator's axis. The temporal response of the output signal was measured on the detector *D* (see Fig. 1) with the use of a beam splitter placed inside the resonator.

The alignment of the resonator was optimized by examining the intensity of the seeding beam after a single pass inside the resonator and then after multiple passes. Before each new measurement, we erased the remaining grating by uniform light illumination of the crystal.

First we optimized the ratio of seeding- to pump-beam intensity to achieve the highest amplification. For the weakest seeding-beam intensity (16 μW), for which the seeding/pump ratio was extremely low, $r_0\sim10^{-4}$, we found the highest gain G (intensity of the resonator beam versus seeding-beam intensity) irrespective of the pump-beam incidence angle. This effect is in agreement with the well-known stan-

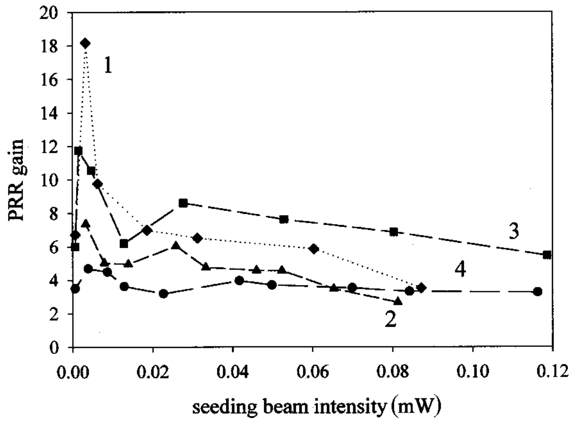

FIG. 2. The measured amplification of the resonator beam inside the resonator as a function of intensity of the injected seeding beam for different pump incident angles: 1, 19°; 2, 30°; 3, 45°; 4, 55°. The amplification factor is taken as the ratio of the measured resonator output to the input seeding-beam intensity.

dard TBC theory, where the TBC gain increases for decreasing seed-to-pump beam ratios (r_0) until saturation. The TBC gain is

$$\frac{1+e^{-\gamma l}}{1+r_0 e^{-\gamma l}} r_0, \tag{15}$$

where l is the interaction length between the two beams inside the crystal.

We also optimized the geometry of the resonator using different pump-beam incident angles (from almost collinear to 55° with the resonator axis). The highest gain was achieved for a 19° pump incidence angle, in agreement with the optimum TBC geometry we established earlier [8]. Results are shown in Fig. 2. The angle between the c axis of the crystal and the resonator axis was kept constant at 41°. Further, we observed the dynamics of resonator-beam buildup and the temporal response of the resonator to the blocking of the seeding beam. In no case did we observe stable photorefractive oscillations. Fast decay of the resonator beam followed blocking of the seeding beam. Decay occurs on the characteristic time scale 0.1–0.3 s. This corresponds to a typical value for the photorefractive time constant [11]. Thus the internal resonator losses are high and the seeding beam provides conditions close to or just above threshold.

We varied the incident angle of the pump beam from almost collinear with the resonator axis to the optimal angle for efficient TBC buildup—around 19°. In some cases the output of the resonator developed well-distinguished temporal modulation as the angle increased. The modulation always started when the resonator beam exceeded the seeding-beam intensity by at least a factor of 2. The period of modulation and the amplitude changed when the angle varied. This phenomenon cannot be explained by spontaneous temperature fluctuations inside the crystal. When the incident pump angle was fixed we observed stable modulation of the output without remarkable changes of average intensity for one-half hour until any temperature instabilities began according to our earlier observations. On the other hand, the parameters of the modulation were reproducible as we moved the angle up and down. We observed a similar dependence of the modulation frequency on the incident pump angle for slight reorientations of the crystal position relative to the resonator axis.

Figure 3 presents the experimental data for the resonator output signal with the seeding beam present. In all plots the measurement starts with both pump and seeding beams incident. After 10–20 min, when a stable oscillation is established, we block the seeding beam, leaving the pump beam on, and observe the temporal decay of the resonator-beam oscillation.

The pictures are taken sequentially as the angle between the resonator axis and pump beam is increased. As can be seen in Figs. 3(b)–3(d), in addition to the steady-state oscillation, there is a periodic behavior with characteristic frequency. After blocking the seeding beam, its interference grating is no longer supported and the resonator oscillation decays rapidly. But the remains of the gratings induced by beam interference can persist after the resonator oscillation has decayed as dark-noise oscillations. This can be referred to as the photorefractive material memory phenomenon. Before starting a new experiment, the remains of the gratings were erased by uniform illumination for 5–10 min.

Following the basic PRR [1] theory, the oscillation conditions for a unidirectional ring resonator depend on the two-wave coupling efficiency γl, which varies for a rotating crystal with respect to the pumping and oscillating beams. The resonator beam appears shifted in the frequency compared to the pump beam. The magnitude of the frequency detuning exhibits a straightforward cavity-length dependence. Previous experiments [1–6] as well as ours have shown that this frequency mismatch may be much less than 1 Hz and is coupled with the resonator parameters.

From the PRR theory of a photorefractive resonator the condition on the frequency mismatch is

$$\Delta\omega \leqslant (1/\tau)(\gamma l/\alpha - 1)^{1/2}, \tag{16}$$

where τ is a photorefractive-intensity-dependent constant and α represents the total losses inside the resonator. As was mentioned earlier [1], the maximum frequency differences near the oscillation threshold are much less than for high gain. Equation (16) reflects the quantitative trend of this effect.

In Fig. 4 we present experimental data for the frequency of modulation as a function of PRR gain for two different crystal orientations relative to the resonator axis. The difference between data points 1 and 2 in Fig. 4 is a slight increase (5°–6°) in the angle between the c axis of the crystal and the resonator axis, which affects the interaction length l inside the crystal and the coupling efficiency. On average the frequency difference is 10 mHz. Although the interpretation of the experimental results using Eqs. (15) and (16) is not straightforward, the quantitative agreement is clear. Crystal reorientation alters TBC efficiency. As a result it affects the maximum frequency difference. Variation of the pump inci-

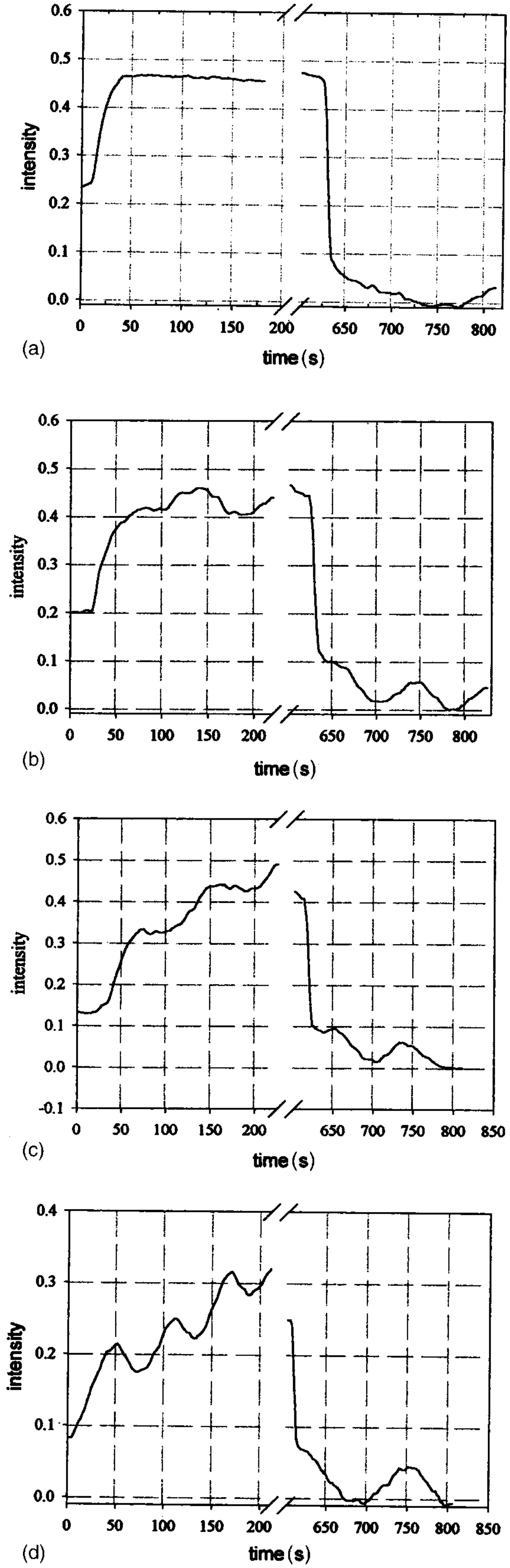

FIG. 3. Temporal evolution of the resonator beam shows the buildup and decay of the resonator oscillation when the seeding is turned off: (a) stationary output; (b)–(d) periodic output.

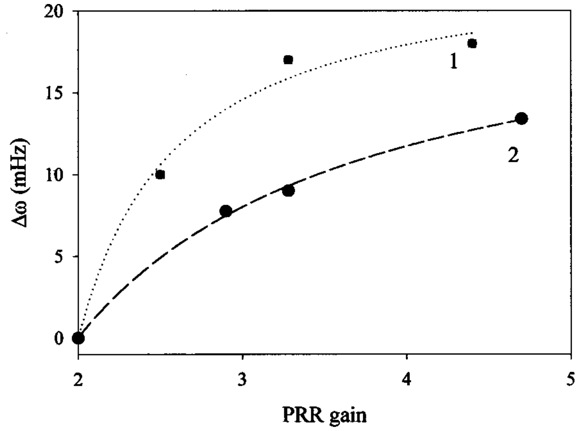

FIG. 4. The modulation frequency as a function of PRR gain (or pump incident angle) for two different orientations of the crystal relative to the resonator axis.

dent angle coupled with TBC has the same effect on the frequency difference. Also, the photorefractive time τ was not constant but varied as the PRR gain changed with increasing incident pump angle. Unfortunately, the experimental parameters are interdependent, which makes a theoretical interpretation difficult. Despite this, our experiments proved that periodic behavior is connected to the resonator configuration. These periodic variations in intensity can be understood from the effect of induced grating competition. The injected external beam forms one grating with the pump beam that is stationary (Q_2) and another that is moving (Q_1), as explained in the previous section. The relative strength of the two grating amplitudes varies as the resonator-beam intensity grows and can be modeled by Eq. (10). The resonator beam diffracts on both gratings, and if the oscillating amplitude Q_1 is strong enough a periodic variation in the diffracted resonator-beam intensity can be observed. When the pump beam is switched off, the grating will start to decay, but its effect on the resonator's intensity can persist for some time. In some cases, the strength of the temporal grating is small as compared with the stationary pattern and that gives a stable output [Fig. 3(a)]. There may be a certain similarity of this device with a multimode laser oscillator. But, as opposed to the two-mode operation of such a laser, where one normal mode actually suppresses oscillation of the other, the ring resonator in the stationary regime tends to lock to the external frequency, due to the small frequency mismatch between the beams.

We have carried out a theoretical analysis of a photorefractive ring resonator injected with an additional seeding beam that originates from the same laser as the pump beam. The expression for the output resonator beam consists of two main contributions: a stationary grating and a grating that oscillates in time with the frequency difference between the pump beam and self-induced cavity oscillations. We have shown that the grating competition will cause periodic variation in intensity of the output resonator beam. This theoretical prediction has been confirmed by our experimental results from a ring resonator containing a Rh:$BaTiO_3$ crystal pumped by a 1.06 μm beam. The strongest resonator beam with periodic oscillations in intensity was achieved with weak seeding beams. In the absence of a seeding beam the PRR did not exhibit stable oscillations. The periodic behavior altered as the resonator parameters varied.

The authors gratefully acknowledge the financial support of the Engineering and Physical Sciences Research Council (EPSRC) under Grant No. GR/M/11844 and of the Royal Society.

[1] P. Yeh, J. Opt. Soc. Am. B **2**, 1924 (1985); M. D. Ewbank and P. Yeh, Opt. Lett. **10**, 496 (1985).
[2] G. D'Alessandro, Phys. Rev. A **46**, 2791 (1992).
[3] Z. Chen, D. McGee, and N. Abraham, J. Opt. Soc. Am. B **13**, 1482 (1996).
[4] G. Balzer, C. Benz, O. Knaup, and T. Tschudi, Chaos, Solitons Fractals **10**, 725 (1999).
[5] Zhuang Jun and Tan Weihan, Phys. Rev. A **54**, 5201 (1996).
[6] J. Leonardy, M. Belic, and F. Kaiser, J. Opt. Soc. Am. B **15**, 1714 (1998).
[7] W. Krolikowski, Bo Su Chen, and M. Cronin-Golomb, J. Opt. Soc. Am. B **8**, 1455 (1991).
[8] M. Kaczmarek and R. W. Eason, Opt. Commun. **154**, 334 (1998).
[9] M. Sargent III, M. O. Scally, and W. E. Lamb, Jr., *Laser Physics* (Addison-Wesley, Reading, MA, 1974).
[10] N. V. Kukhtarev, V. Markov, and S. Odulov, Opt. Commun. **23**, 338 (1977).
[11] B. M. Jost and B. E. A. Saleh, J. Opt. Soc. Am. B **11**, 1864 (1994).
[12] D. Z. Anderson and R. Saxena, J. Opt. Soc. Am. B **4**, 164 (1987).